

Analysis of Mean Shortest Path Lengths in the Stochastic Subscriber Line Model

Hendrik Schmidt

Joint work with F. Fleischer, C. Gloaguen and V. Schmidt

University of Ulm

Department of Stochastics

France Télécom, Division R&D, Paris

Outline

- **Stochastic–geometric network modelling**
 - Real network data
 - Stochastic Subscriber Line Model
 - Geometry Model, Equipment Model, Topology Model

Outline

- **Stochastic–geometric network modelling**
 - Real network data
 - Stochastic Subscriber Line Model
 - Geometry Model, Equipment Model, Topology Model
- **Neveu's Exchange Formula for Palm Distributions**

Outline

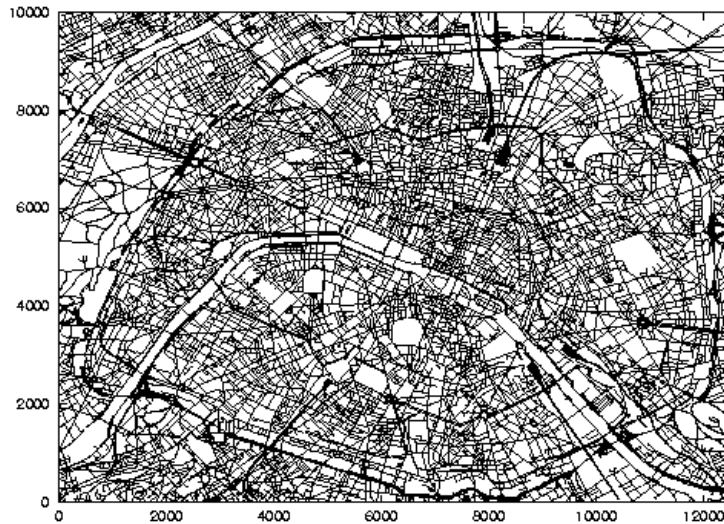
- **Stochastic–geometric network modelling**
 - Real network data
 - Stochastic Subscriber Line Model
 - Geometry Model, Equipment Model, Topology Model
- **Neveu's Exchange Formula for Palm Distributions**
- **Mean shortest path lengths**
 - Simulation methods
 - Application of Neveu
- **Mean subscriber line lengths**

Outline

- **Stochastic–geometric network modelling**
 - Real network data
 - Stochastic Subscriber Line Model
 - Geometry Model, Equipment Model, Topology Model
- **Neveu's Exchange Formula for Palm Distributions**
- **Mean shortest path lengths**
 - Simulation methods
 - Application of Neveu
- **Mean subscriber line lengths**
- **Numerical examples**

Stochastic–geometric network modelling

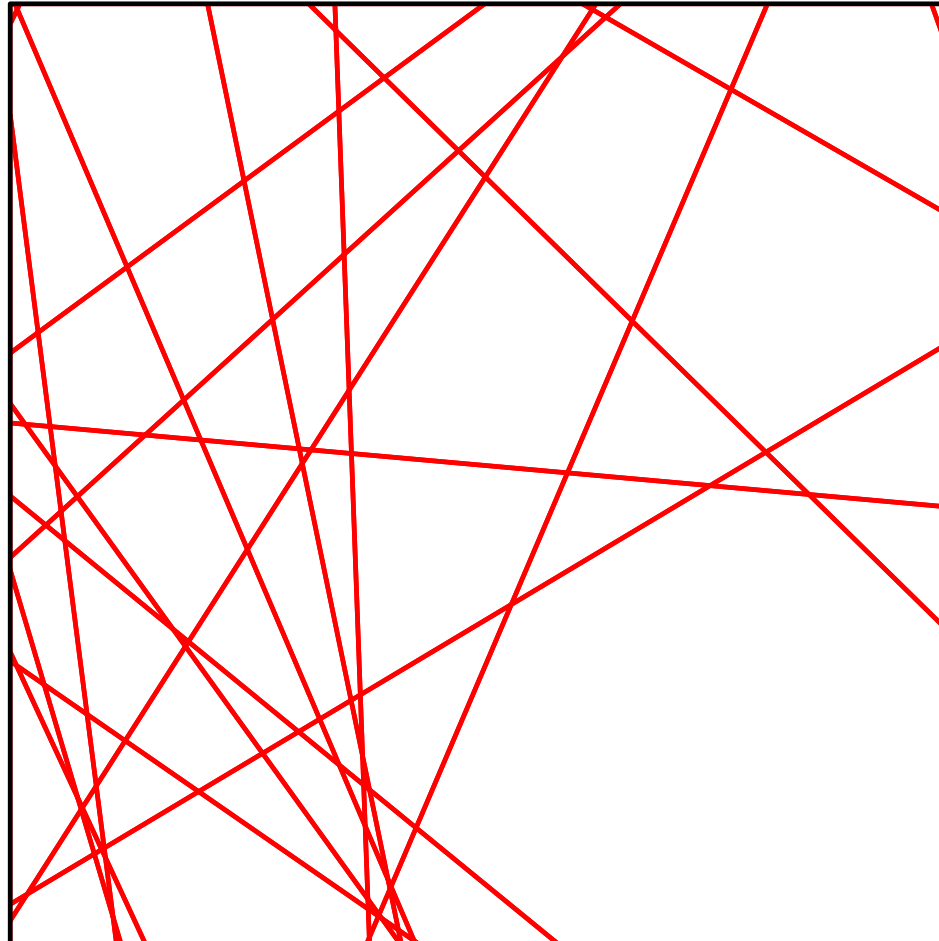
Real network data



Infrastructure system of Paris

Stochastic–geometric network modelling

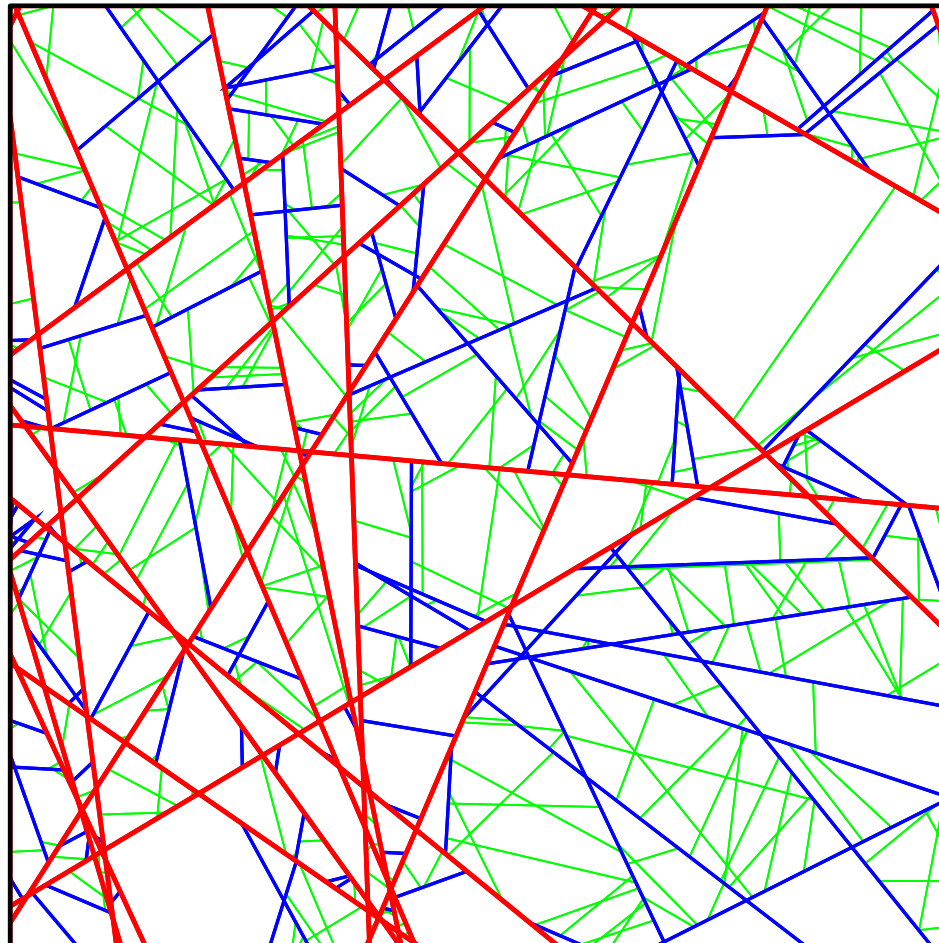
Stochastic Subscriber Line Model



Main roads

Stochastic–geometric network modelling

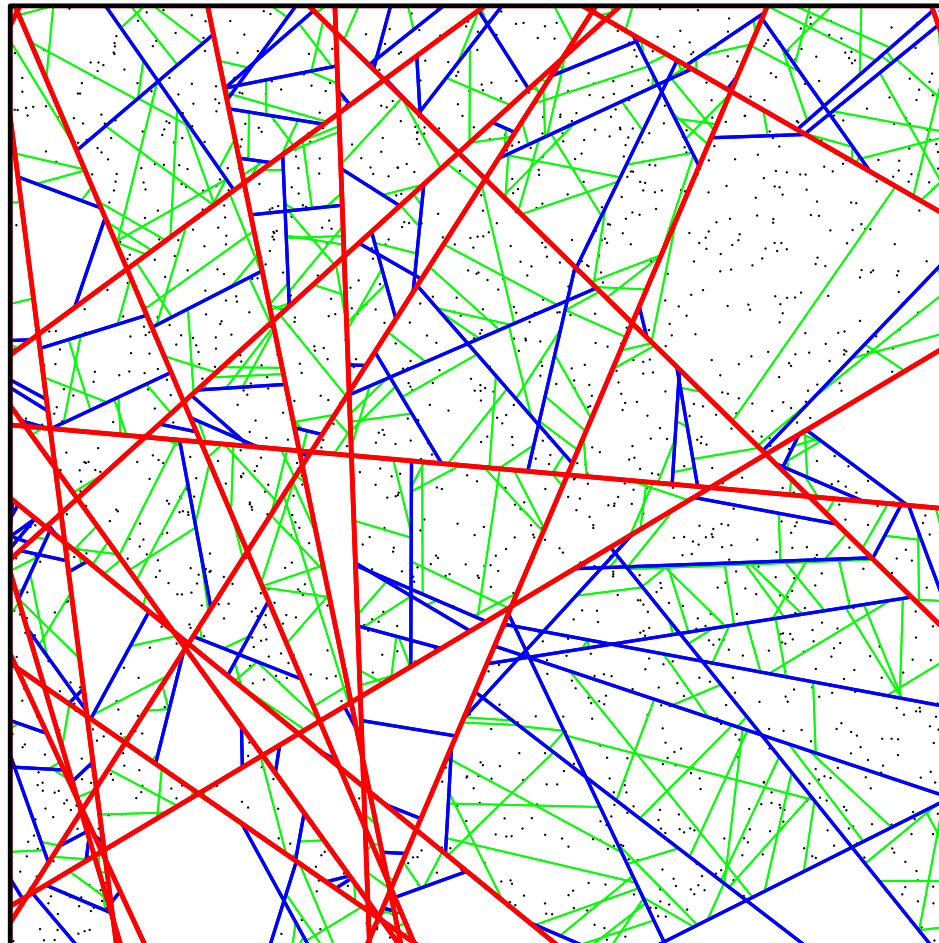
Stochastic Subscriber Line Model



Main roads and side streets

Stochastic–geometric network modelling

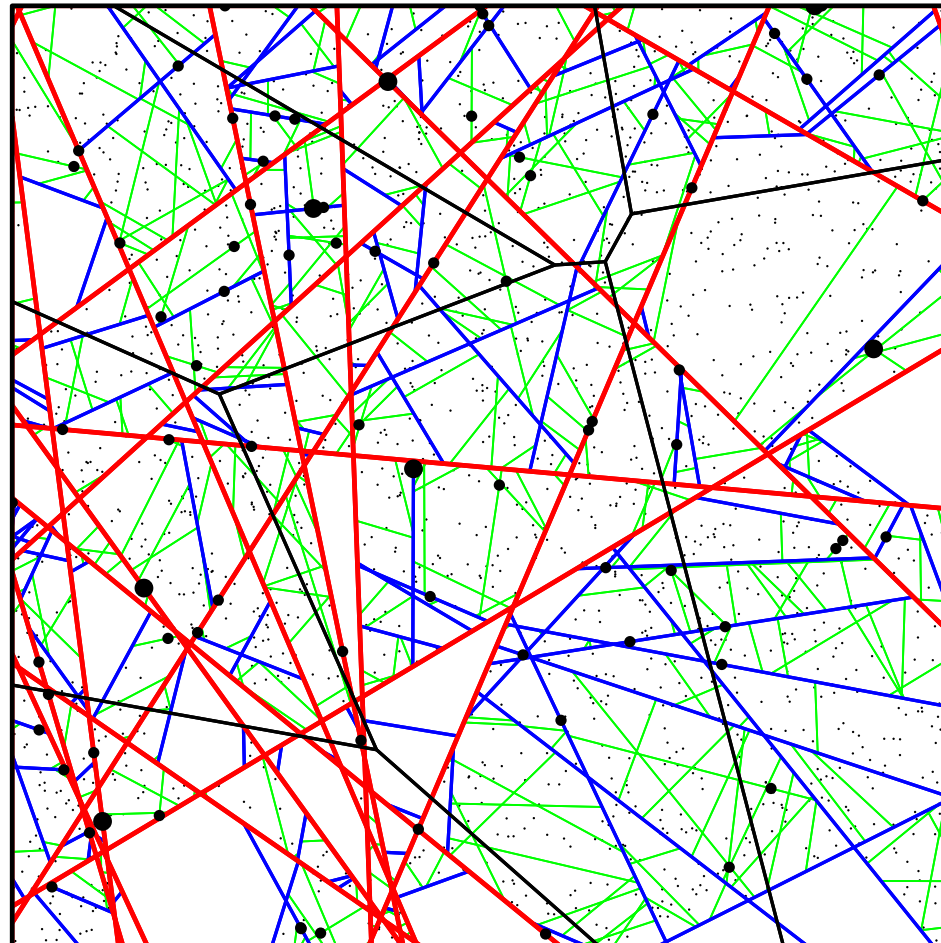
Stochastic Subscriber Line Model



Location of subscribers

Stochastic–geometric network modelling

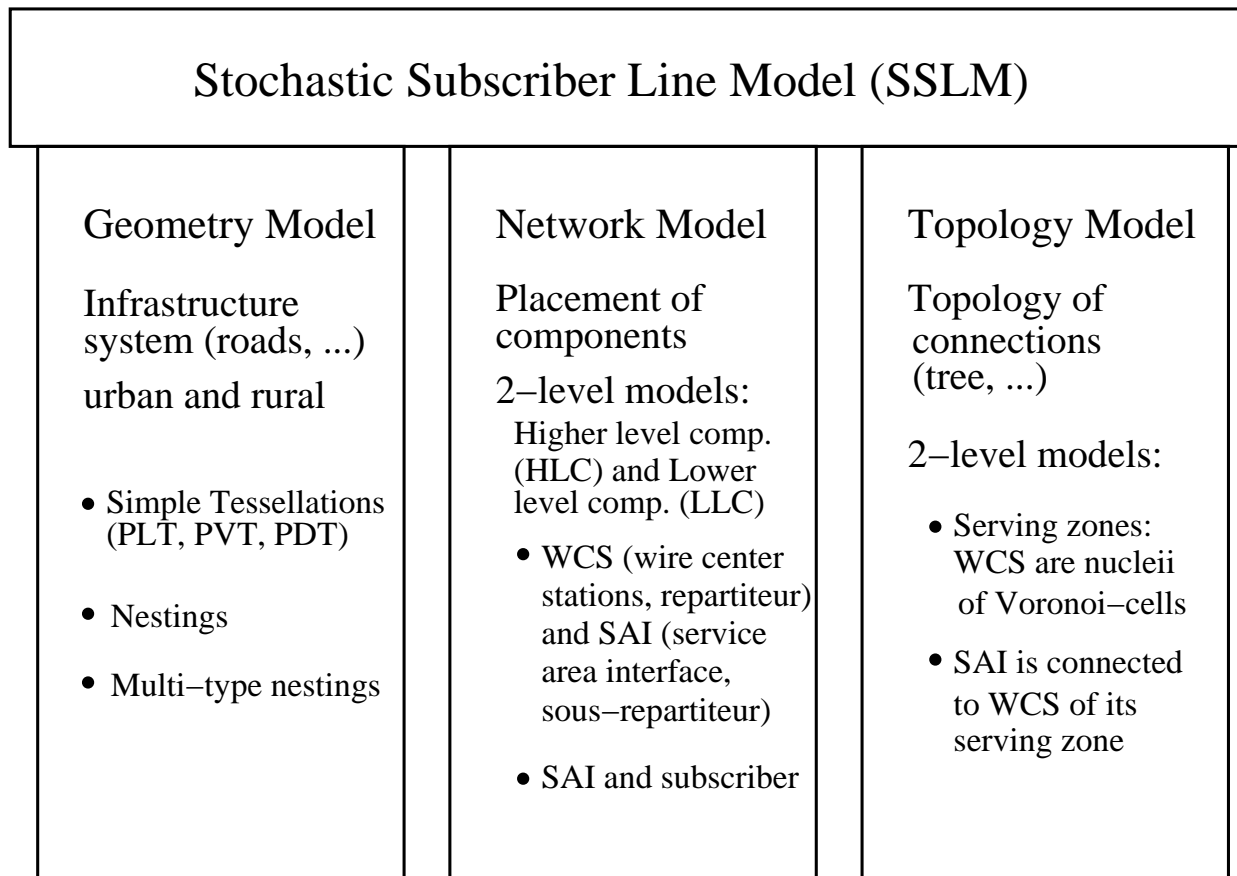
Stochastic Subscriber Line Model



Network nodes and serving zones

Stochastic–geometric network modelling

Stochastic Subscriber Line Model



Neveu's formula

Random point processes

- Mapping $X : \Omega \rightarrow M(\mathbb{R}^2) = M$
 - $(\Omega, \mathcal{A}, \mathbb{P})$: probability space
 - M : Set of simple and locally finite counting measures
- Representations of X
 - **Random counting measure** $\sum_{x \in \text{supp}(X)} \delta_x$
 - Sequence $\{X_n\}_{n \geq 1}$ of **random points**
- **Intensity measure** $\Lambda : \mathcal{B}(\mathbb{R}^2) \rightarrow [0, \infty]$
$$\Lambda(B) = \mathbb{E}X(B), \quad B \in \mathcal{B}(\mathbb{R}^2)$$
- In case of stationarity
 - $\Lambda(B) = \lambda \nu_2(B)$ for $B \in \mathcal{B}(\mathbb{R}^2)$
 - λ is called **intensity**

Neveu's formula

Random marked point processes

- Mapping $X_D : \Omega \rightarrow M(\mathbb{R}^2 \times D) = M_D$
- Representation of X_D
 - Random counting measure
 - Sequence of $\{[X_n, D_n]\}_{n \geq 1}$ random marked points

Neveu's formula

Random marked point processes

- Mapping $X_D : \Omega \rightarrow M(\mathbb{R}^2 \times D) = M_D$
- Representation of X_D
 - Random counting measure
 - Sequence of $\{[X_n, D_n]\}_{n \geq 1}$ random marked points
- Flow $\{\theta_x, x \in \mathbb{R}^2\}$ with $\theta_x : \Omega \rightarrow \Omega$
- Palm distribution $\mathbb{P}_{X_D}^*$ of $X_D : \Omega \rightarrow M_D$,

$$\mathbb{P}_{X_D}^*(A \times G) = \frac{1}{\lambda \nu_2(B)} \int_{\Omega} \int_{\mathbb{R}^2 \times G} \mathbf{1}_B(x) \mathbf{1}_A(\theta_x \omega) X_D(\omega, d(x, g)) \mathbb{P}(d\omega)$$

for $B \in \mathcal{B}(\mathbb{R}^2)$ and $A \in \mathcal{A}$, $G \in \mathcal{B}(D)$, $0 < \lambda < \infty$

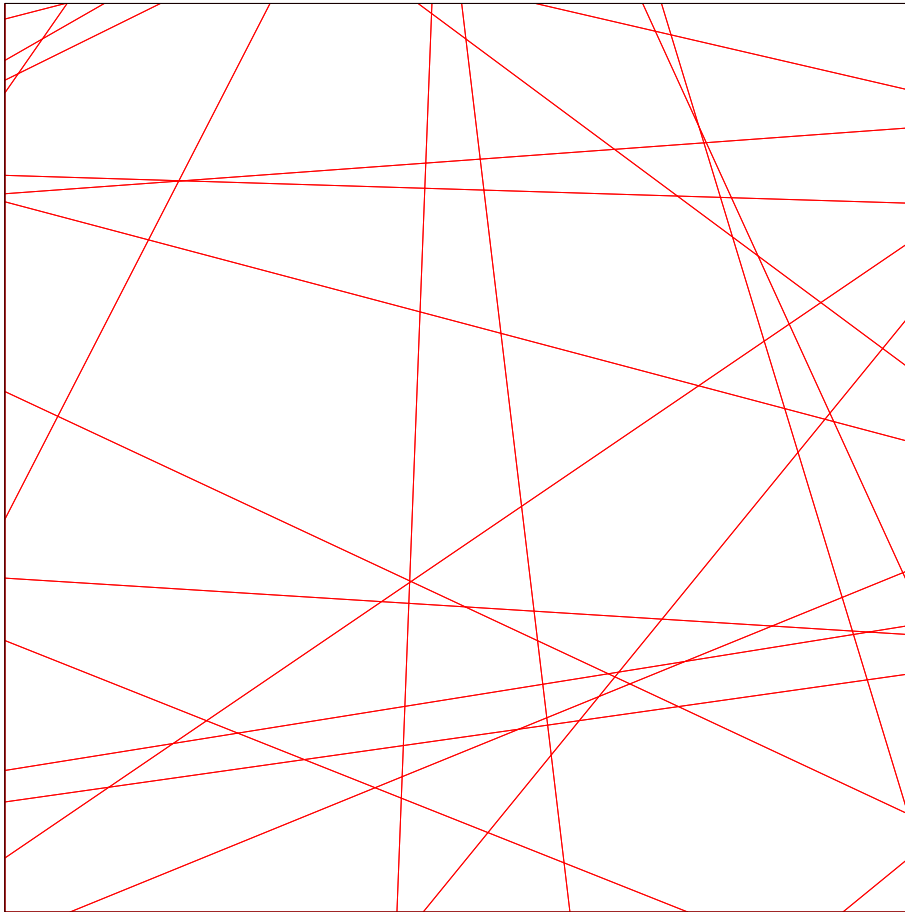
Neveu's formula

For any measurable function $f : \mathbb{R}^2 \times D \times \tilde{D} \times \Omega \rightarrow [0, \infty)$

$$\begin{aligned} & \lambda \int_{\Omega \times D} \int_{\mathbb{R}^2 \times \tilde{D}} f(x, g, \tilde{g}, \theta_x \omega) \tilde{X}_{\tilde{D}}(\omega, d(x, \tilde{g})) \mathbb{P}_{X_D}^*(d(\omega, g)) \\ &= \tilde{\lambda} \int_{\Omega \times \tilde{D}} \int_{\mathbb{R}^2 \times D} f(-x, g, \tilde{g}, \omega) X_D(\omega, d(x, g)) \mathbb{P}_{\tilde{X}_{\tilde{D}}}^*(d(\omega, \tilde{g})) \end{aligned}$$

Model description

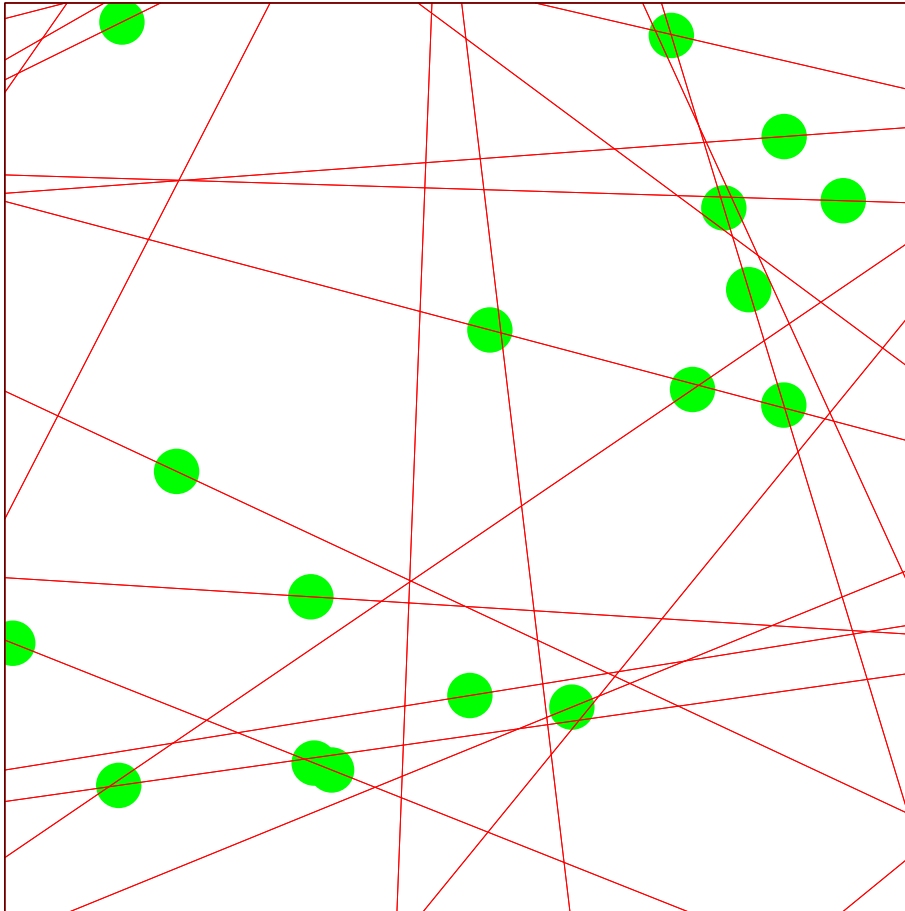
Geometry model



- Poisson line tessellation X_ℓ
- Intensity $\gamma > 0$:
Mean total length of lines per unit area

Model description

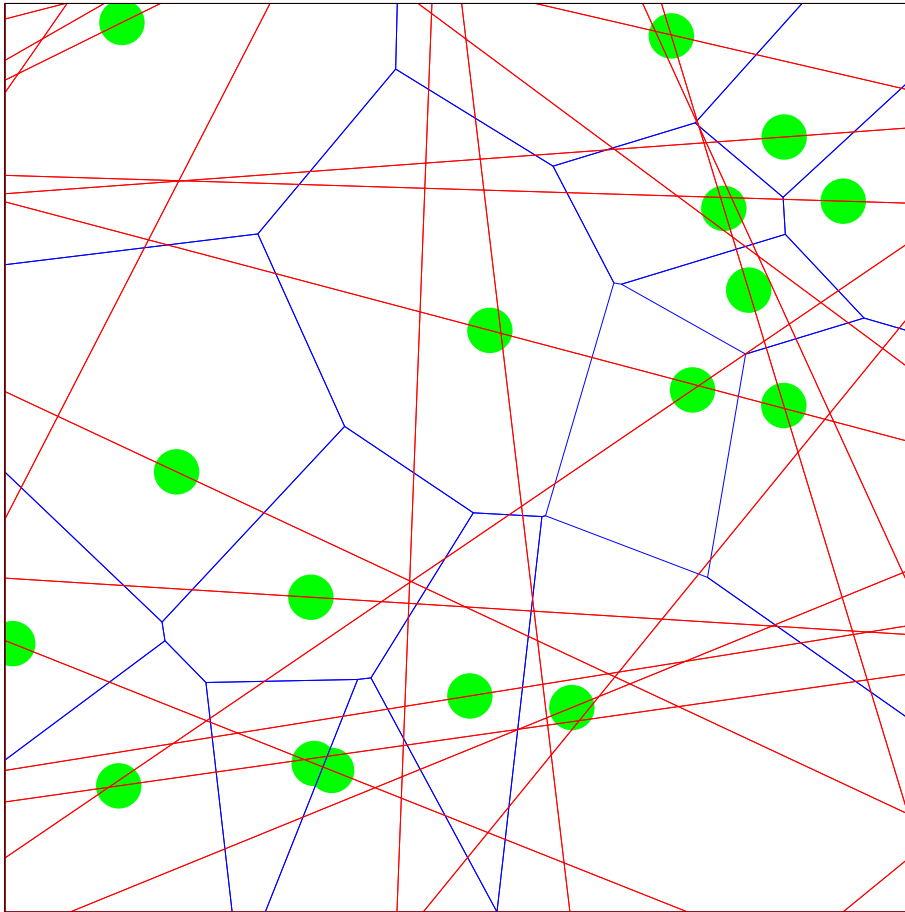
Placement of higher level components



- Stationary ergodic point process
 $X_H = \{X_n\}_{n \geq 1}$ on the lines
- Special case: Poisson process
 X_H
- Linear intensity
 $\lambda_1 > 0$
- Planar intensity
 $\lambda_H = \gamma \lambda_1$

Model description

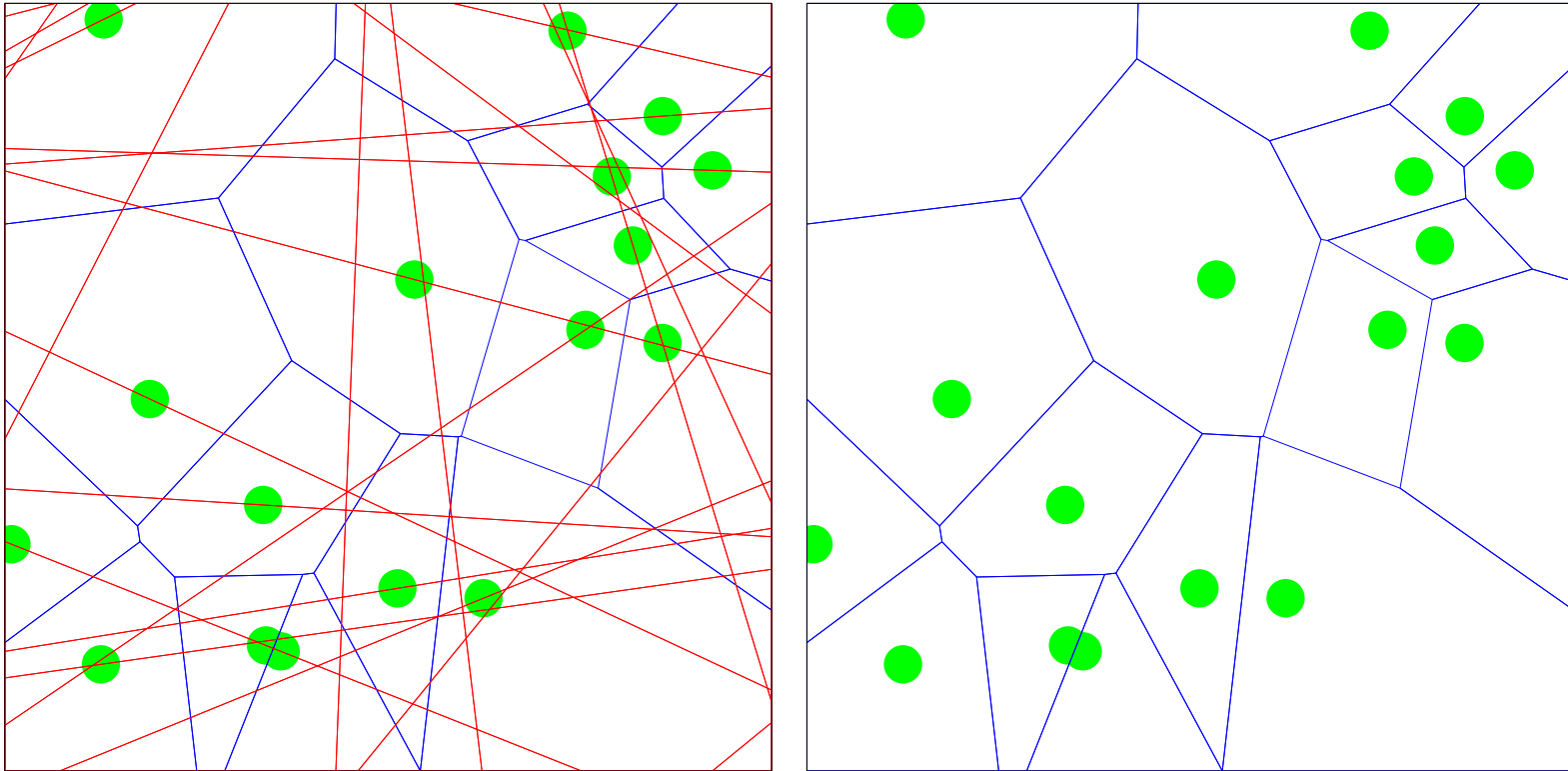
Serving zones



- Sequence of serving zones $\{\Xi(X_n)\}_{n \geq 1}$
- Later on:
 - Typical serving zone Ξ^*
 - Typical line system $L(\Xi^*)$

Model description

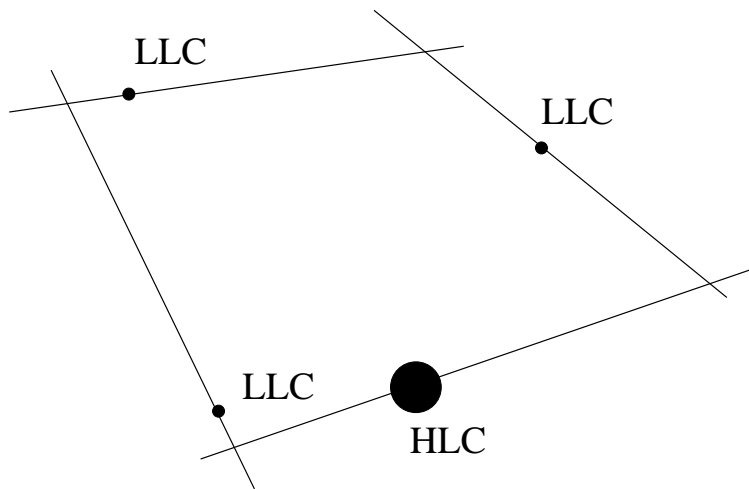
Serving zones



Cox-Voronoi tessellation (CVT) based on a Poisson line process

Mean shortest path lengths

Placement of lower level components



Linear placement on lines

- Stationary Poisson process $\{\tilde{X}_n\}_{n \geq 1}$ on the lines
- Linear intensity $\lambda_2 > 0$
- Planar intensity $\lambda_L = \gamma \lambda_2$
- Stationary marked point process $X_L = \{[\tilde{X}_n, c(P(\tilde{X}_n, N(\tilde{X}_n)))]\}_{n \geq 1}$
- $N(\tilde{X}_n)$ location of nearest HLC of \tilde{X}_n
- $P(\tilde{X}_n, N(\tilde{X}_n))$ shortest path from \tilde{X}_n to $N(\tilde{X}_n)$
- $c(P(\tilde{X}_n, N(\tilde{X}_n)))$ length (costs) of $P(\tilde{X}_n, N(\tilde{X}_n))$

Mean shortest path lengths

Simulation methods

- Natural Approach

- Simulate network in (large) sampling window $W \subset \mathbb{R}^2$
- Compute $c(P(\tilde{X}_n, N(\tilde{X}_n)))$ for each \tilde{X}_n
- Compute **mean shortest path length**

$$c_{LH}(W) = \frac{1}{\#\{n : \tilde{X}_n \in W\}} \sum_{n \geq 1} \mathbb{I}_W(\tilde{X}_n) c(P(\tilde{X}_n, N(\tilde{X}_n)))$$

- Disadvantages

- W small \Rightarrow edge effects significant
- W large \Rightarrow memory and runtime problems

Mean shortest path lengths

Simulation methods

- Alternative Approach
 - $\{W_i\}_{i \geq 1}$ averaging sequence of sampling windows
 - Ergodicity of X_L yields with probability 1 that

$$\lim_{i \rightarrow \infty} c_{LH}(W_i) = c_{LH}^*$$

The limit c_{LH}^* is given by ($B \in \mathcal{B}_0(\mathbb{R}^2)$)

$$\frac{1}{\lambda_L \nu_2(B)} \mathbf{E} \sum_{n \geq 1} \mathbf{1}_B(\tilde{X}_n) c(P(\tilde{X}_n, N(\tilde{X}_n))) = \mathbf{E}_{X_L} c(P(o, N(o)))$$

- Disadvantages
 - Simulation not clear
 - Not very efficient

Mean shortest path lengths

- Application of Neveu



$$\mathbb{E}_{X_L} c(P(o, N(o))) = \frac{1}{\mathbb{E}_{X_H} \nu_1(L(\Xi^*))} \mathbb{E}_{X_H} \int_{L(\Xi^*)} c(P(u, o)) du$$

- With

$$\frac{1}{\mathbb{E}_{X_H} \nu_1(L(\Xi^*))} = \lambda_1$$

- Independence from λ_2
- Simulation algorithm for typical cell of CVT needed

Mean shortest path lengths

Computational algorithm

Estimators for c_{LH}^* ($k \geq 1$),

•

$$\hat{c}_{LH}(k) = \frac{1}{\sum_{i=1}^k \nu_1(L(\Xi_i^*))} \sum_{i=1}^k \sum_{j=1}^{M_i} \int_{S_i^{(j)}} c(P(u, o)) du$$

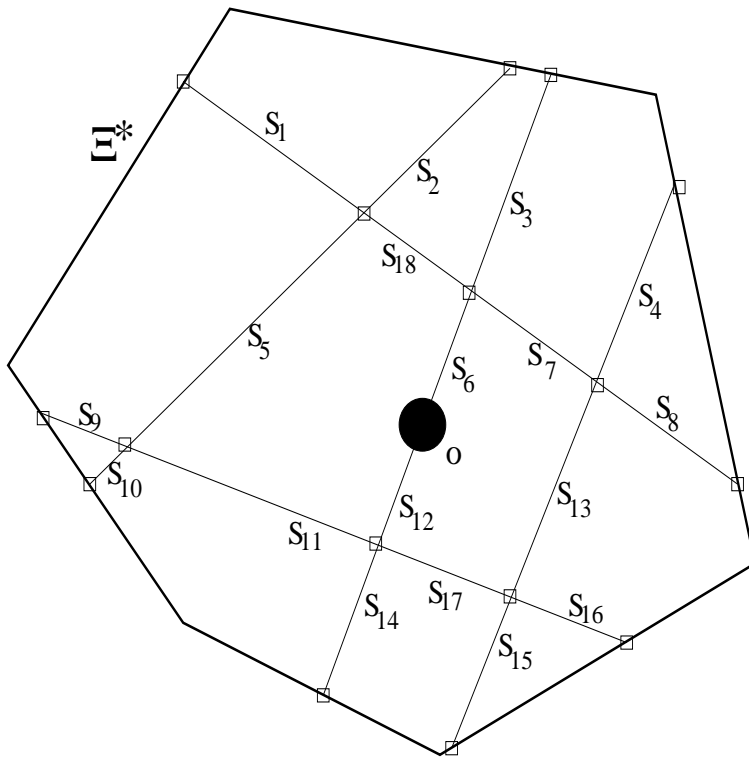
•

$$\check{c}_{LH}(k) = \lambda_1 \frac{1}{k} \sum_{i=1}^k \sum_{j=1}^{M_i} \int_{S_i^{(j)}} c(P(u, o)) du$$

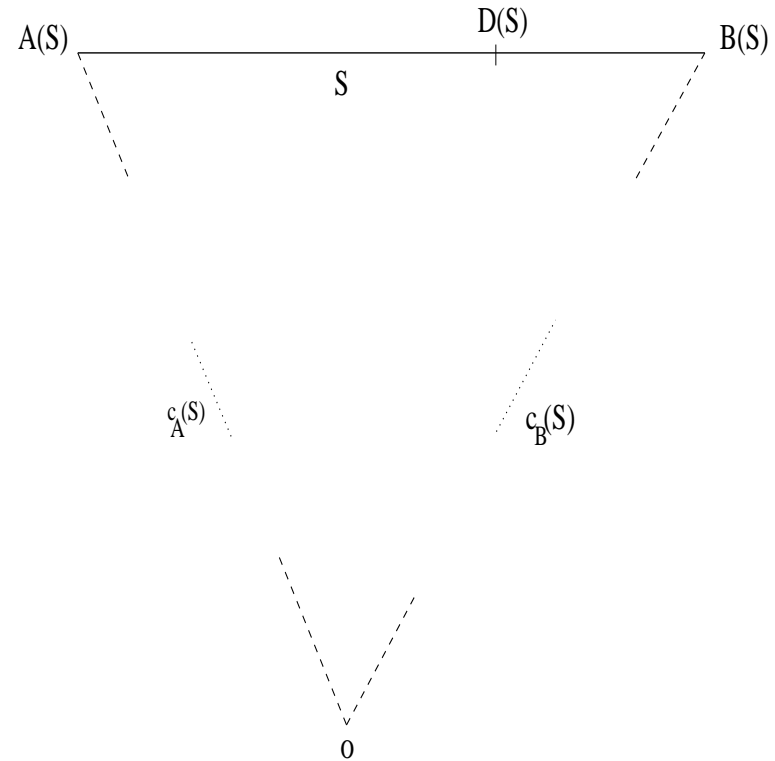
• $\int_{S_i^{(j)}} c(P(u, o)) du$ can be analytically calculated

Mean shortest path lengths

Computational algorithm



Partitioning of $L(\Xi^)$ into segments*

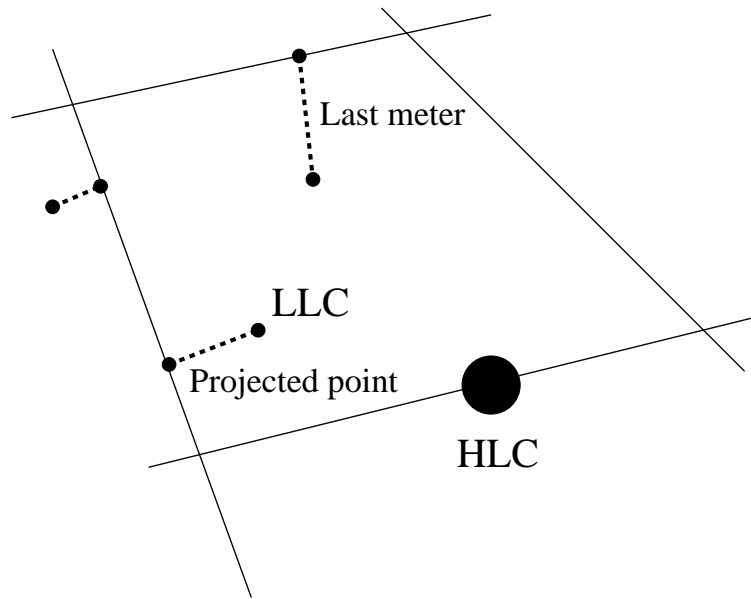


Mean shortest path length for S

$$\int_S c(P(u, o)) du = \frac{1}{4}(\nu_1(S))^2 + \frac{1}{2}(c_A(S) + c_B(S))\nu_1(S) + \frac{1}{4}(c_B(S) - c_A(S))^2$$

Mean subscriber line lengths

Placement of lower level components



Spatial placement and projection to nearest line

- Stationary Poisson point process $\{X'_n\}_{n \geq 1}$ (int. λ_L)
- Stationary marked point process $X'_L = \{[X'_n, c(P(X'_n, N(X'_n)))]\}_{n \geq 1}$
- $N(X'_n)$ location of nearest HLC of X'_n
- Project X'_n onto X''_n
- $c(P(X'_n, N(X'_n))) = c'(X'_n, X''_n) + c(P(X''_n, N(X'_n)))$
- $c'(X'_n, X''_n)$ cost value of last meter

Mean subscriber line lengths

Simulation methods

- **Mean subscriber line length**

$$d_{LH}(W) = \frac{1}{\#\{n : X'_n \in W\}} \sum_{n \geq 1} \mathbb{1}_W(X'_n) c(P(X'_n, N(X'_n)))$$

- **Ergodicity of X'_L**

$$\lim_{i \rightarrow \infty} d_{LH}(W_i) = d_{LH}^* = \mathbb{E}_{X'_L} c(P(o, N(o)))$$

Mean subscriber line lengths

Simulation methods

- **Mean subscriber line length**

$$d_{LH}(W) = \frac{1}{\#\{n : X'_n \in W\}} \sum_{n \geq 1} \mathbb{1}_W(X'_n) c(P(X'_n, N(X'_n)))$$

- **Ergodicity of X'_L**

$$\lim_{i \rightarrow \infty} d_{LH}(W_i) = d_{LH}^* = \mathbb{E}_{X'_L} c(P(o, N(o)))$$

- **Application of Neveu**

$$\mathbb{E}_{X'_L} c(P(o, N(o))) = \frac{1}{\mathbb{E}_{X_H} \nu_2(\Xi^*)} \mathbb{E}_{X_H} \int_{\Xi^*} c(P(u, o)) du$$

Mean subscriber line lengths

Computational algorithm

Estimators for d_{LC}^* ($k \geq 1$),

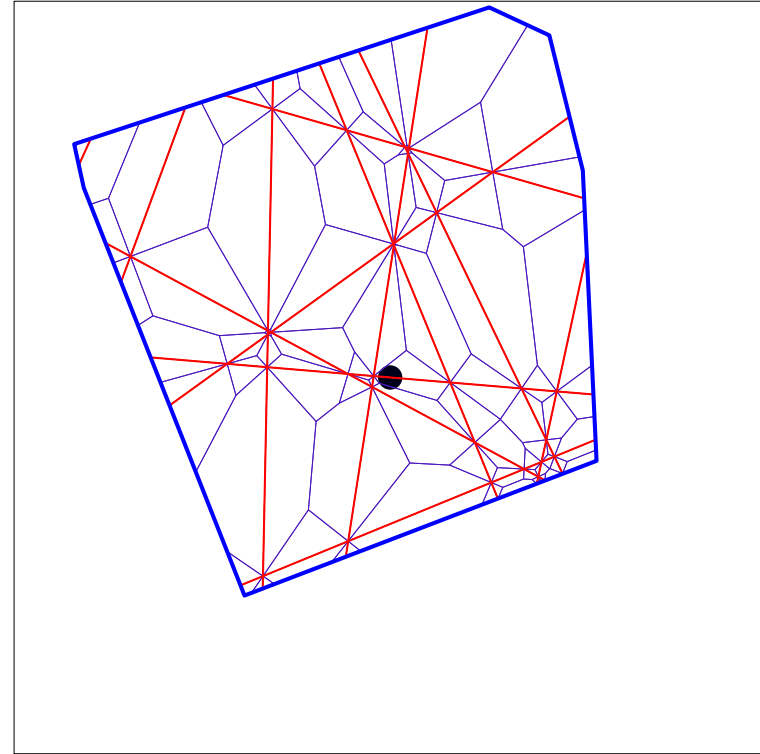
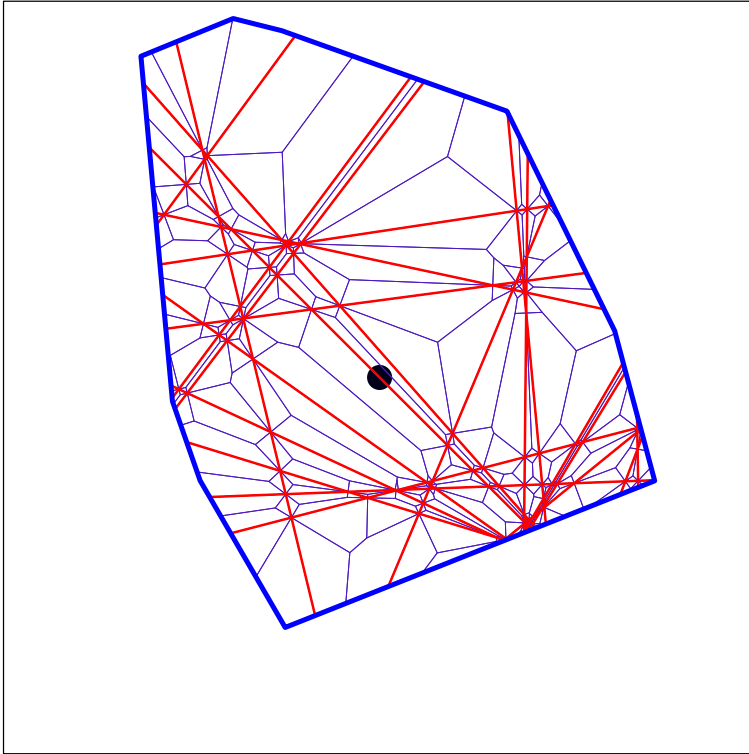
- $$\hat{d}_{LH}(k) = \frac{1}{\sum_{i=1}^k \nu_2(\Xi_i^*)} \sum_{i=1}^k \sum_{j=1}^{K_i} \int_{\Psi_i^{(j)}} c(P(u, o)) du$$

- $$\check{d}_{LH}(k) = \lambda_1 \gamma \frac{1}{k} \sum_{i=1}^k \sum_{j=1}^{K_i} \int_{\Psi_i^{(j)}} c(P(u, o)) du$$

- $\int_{\Psi_i^{(j)}} c(P(u, o)) du$ can be analytically calculated

Mean subscriber line lengths

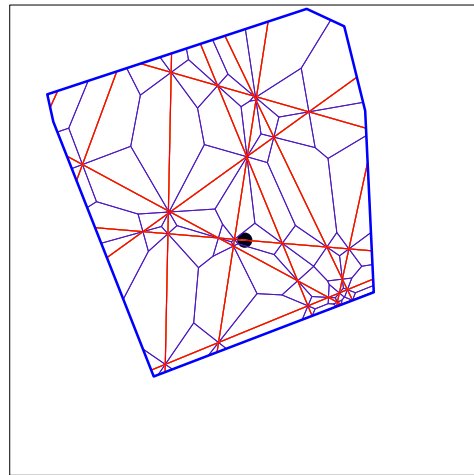
Computational algorithm



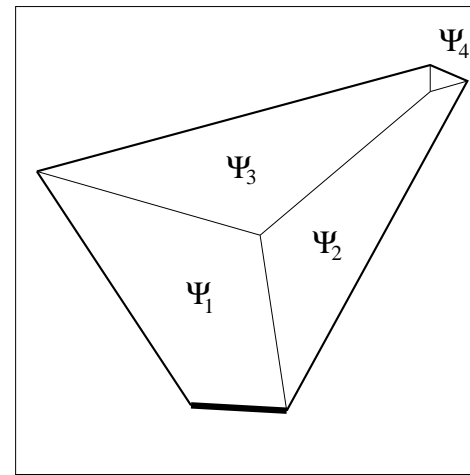
Samples of typical Cox–Voronoi serving zones

Mean subscriber line lengths

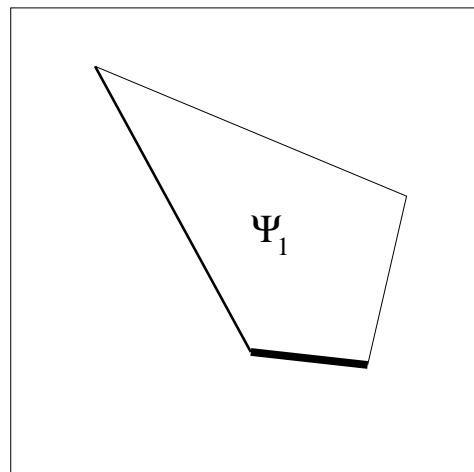
Computational algorithm



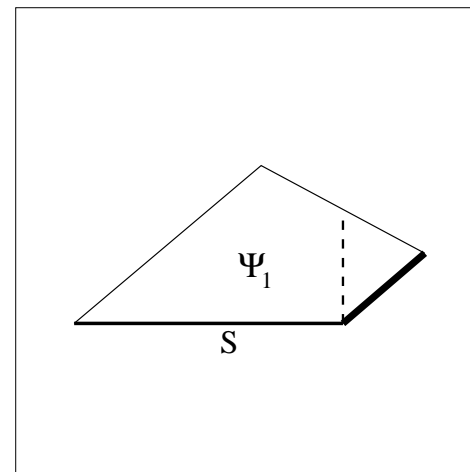
(a) Typical cell



(b) A micro-cell



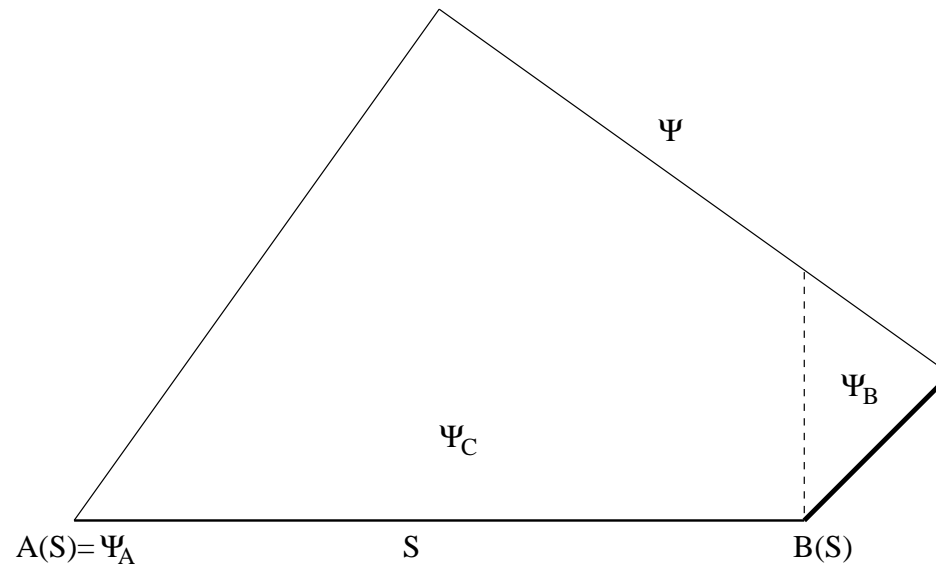
(c) Part of this micro-cell



(d) Further decomposition

Mean subscriber line lengths

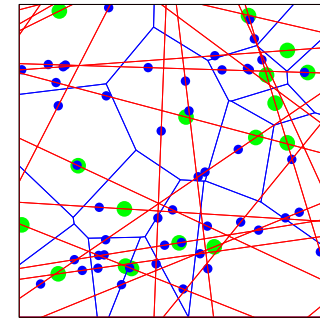
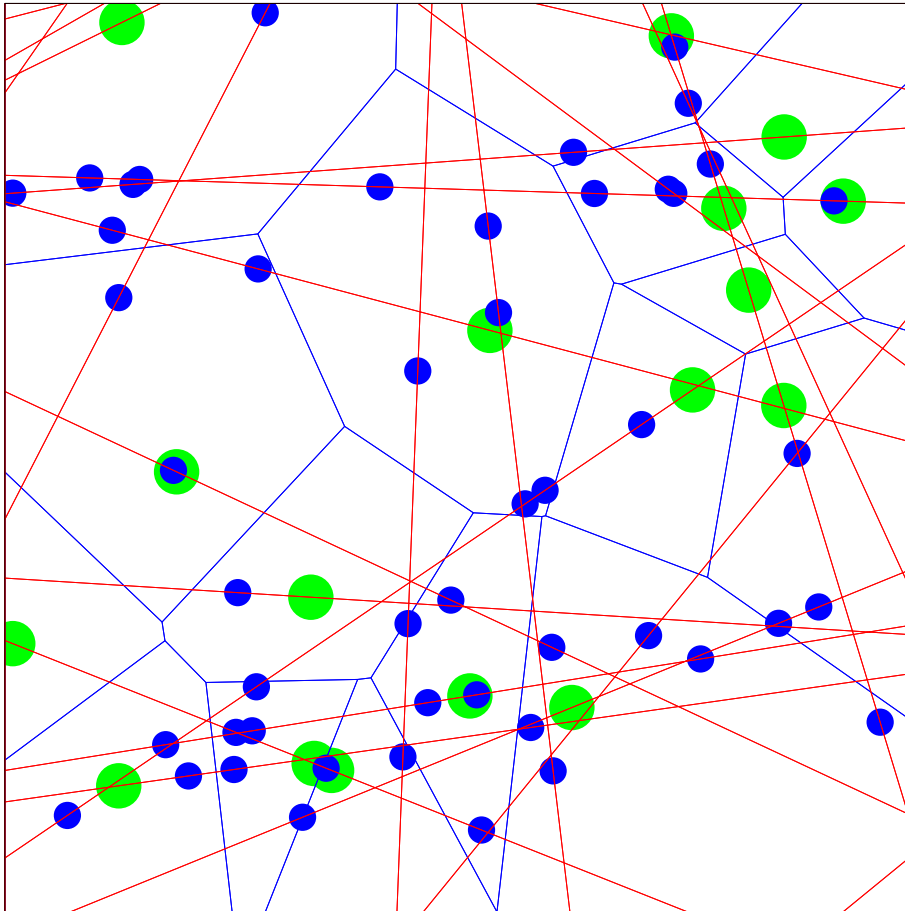
Computational algorithm




$$\int_{\Psi} c(P(u, o)) du = c_a(S) \nu_2(\Psi_A) + c_B(S) \nu_2(\Psi_B) + \int_{\Psi_C} c(P(u, o)) du$$


Numerical results

Scaling property



Let $\gamma^{(1)}/\lambda_1^{(1)} = \gamma^{(2)}/\lambda_1^{(2)}$

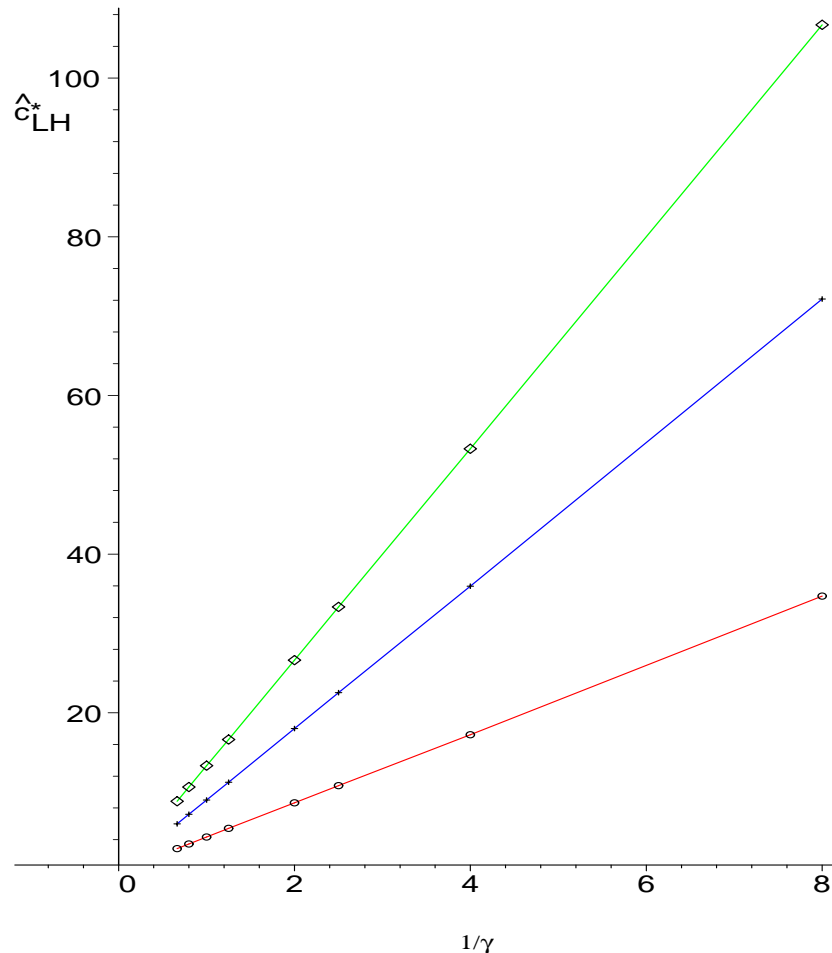
 $\gamma^{(1)} c_{LH}^*(\gamma^{(1)}, \lambda_1^{(1)})$
 $= \gamma^{(2)} c_{LH}^*(\gamma^{(2)}, \lambda_1^{(2)})$

 $\gamma^{(1)} d_{LH}^*(\gamma^{(1)}, \lambda_1^{(1)})$
 $= \gamma^{(2)} d_{LH}^*(\gamma^{(2)}, \lambda_1^{(2)})$

Different intensities but same $\kappa = \gamma/\lambda_1$

Numerical results

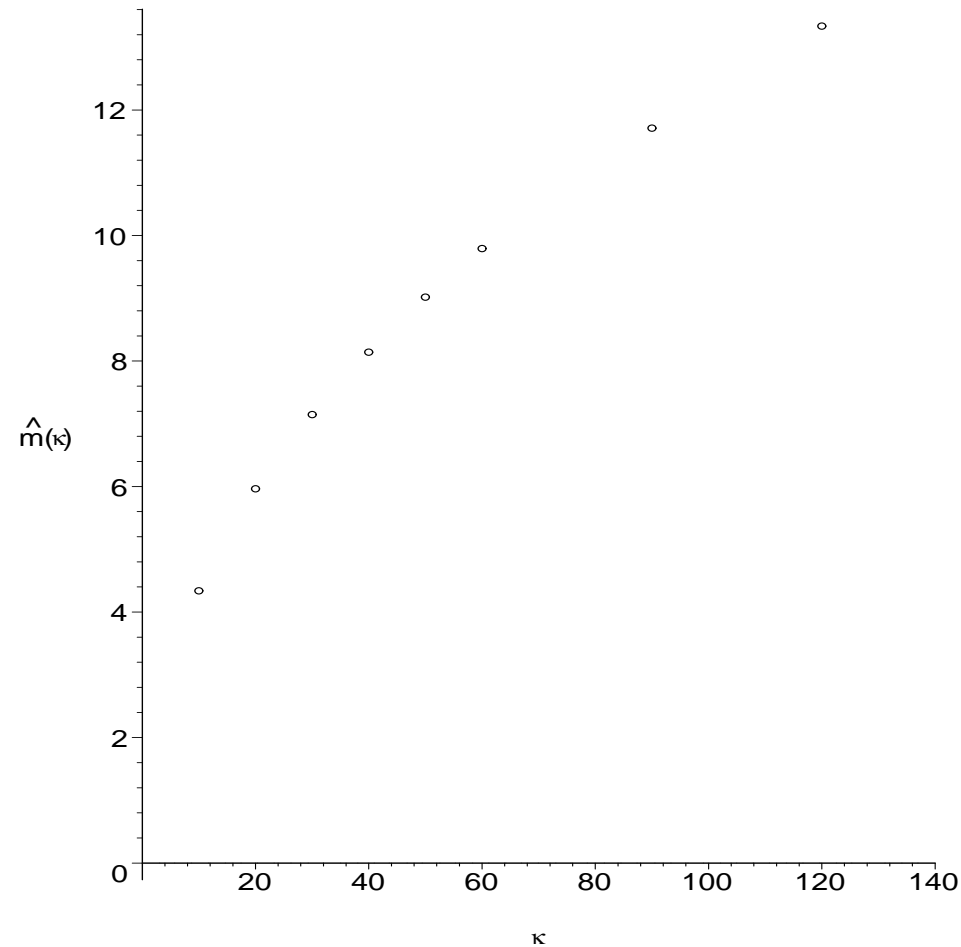
Mean shortest path lengths



- 50000 realizations of Ξ^* (and $L(\Xi^*)$)
- Estimated results of c_{LH}^* for
 - $\kappa = 10$
 - $\kappa = 50$
 - $\kappa = 120$
- $c_{LH}^*(\gamma, \lambda_1) = m(\kappa)/\gamma$

Numerical results

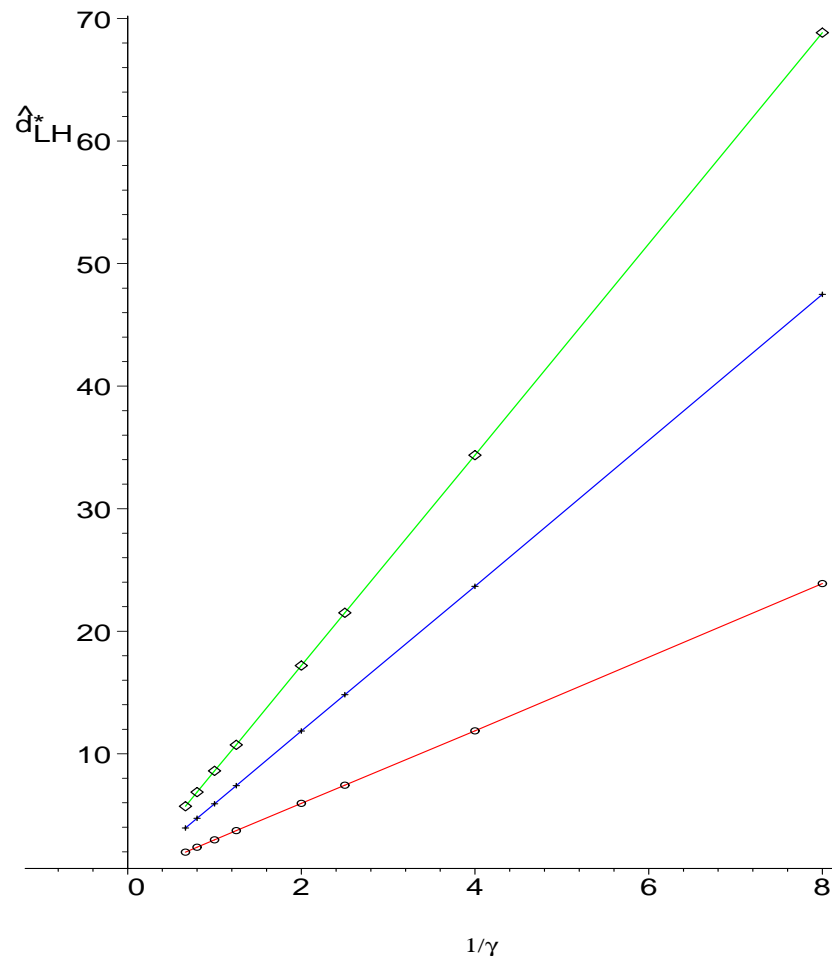
Mean shortest path lengths



$m(\kappa)$ of c_{LH}^* for increasing κ

Numerical results

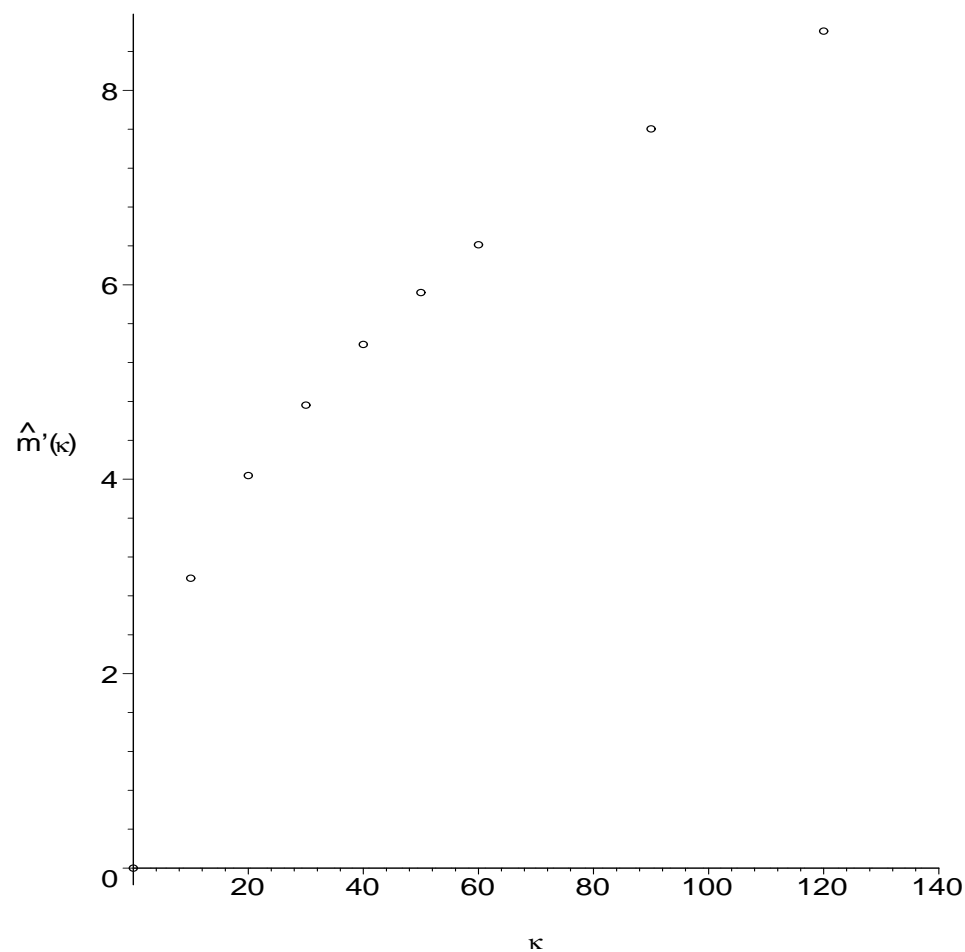
Mean subscriber line lengths



- 50000 realizations of Ξ^* (and $L(\Xi^*)$)
- Estimated results of d_{LH}^* for
 - $\kappa = 10$
 - $\kappa = 50$
 - $\kappa = 120$
- $d_{LH}^*(\gamma, \lambda_1) = m'(\kappa)/\gamma$

Numerical results

Mean subscriber line lengths



$m'(\kappa)$ of d_{LH}^* for increasing κ

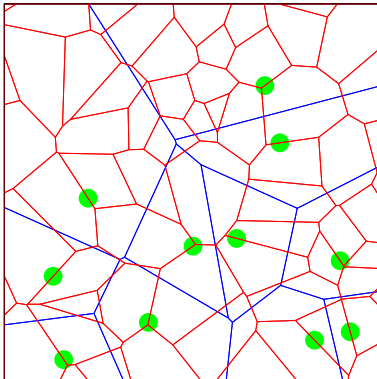
Numerical results

Comparison and Summary

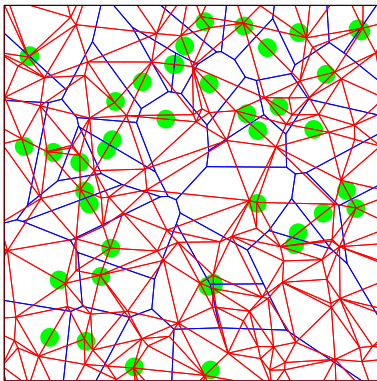
- $c_{LH}^* > d_{LH}^*$ for any parameter pair (λ_1, γ)
- Good approximations $m(\kappa) \approx a\kappa^b$ and $m'(\kappa) \approx a'\kappa^{b'}$
- Thereby estimation of c_{LH}^* and d_{LH}^* without simulation possible
 - $\kappa = \gamma/\lambda_1$
 - $\hat{m}(\kappa) = a\kappa^b$
 - $\hat{m}'(\kappa) = a'\kappa^{b'}$
 - $\hat{c}_{LH}^* = \hat{m}(\kappa)\gamma^{-1}$
 - $\hat{d}_{LH}^* = \hat{m}'(\kappa)\gamma^{-1}$

Outlook

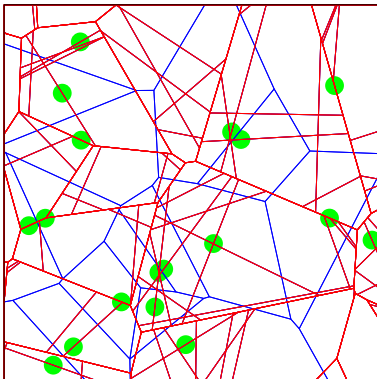
Extensions to other geometry models



CVT based on Poisson-Voronoi



CVT based on Poisson-Delaunay



CVT based on iterated tessellations

Literature

- C. Gloaguen, F. Fleischer, H. Schmidt, V. Schmidt.
Simulation of typical Cox-Voronoi cells, with a special regard to implementation tests.
Mathematical Methods of Operations Research 62(3), 357-373 (2005).
- C. Gloaguen, F. Fleischer, H. Schmidt, V. Schmidt.
Analysis of shortest path and subscriber line lengths in telecommunication access networks.
Preprint, (2005).
- For more information www.geostoch.de